

Enhancing Theoretical Efficiency of Solar Cells: From Single-Junction Fundamentals to Down-Conversion Integrated Multijunction Architectures and Future Prospects for Up-Conversion

Yanming Lui

Abstract

In this work, we propose and analyze a new photovoltaic architecture, the down-converting multijunction (DC-MJ) solar cell, and explore the potential for further efficiency gains through the inclusion of up-conversion layers. Using a detailed balance framework and a differential evolution optimization algorithm, we determine the maximum theoretical efficiencies for various configurations. Our model finds a theoretical peak efficiency of 63.8%, exceeding the Shockley-Queisser limit and surpassing conventional MJ cells. Lastly, we discuss the potential engineering and fabrication challenges associated with creating such hybrid devices and suggest future directions for research. With continued progress in material synthesis and photonic engineering, these hybrid architectures could provide a pathway toward the next generation of ultra-high-efficiency photovoltaics.

1 Introduction

Solar cells are one of the most important sources of renewable energy for society, capable of harnessing the most abundant source of energy on the planet – sunlight. However, solar cells still face numerous problems that prevent them from reaching their full potential. One of the most fundamental limitations is that traditional single-junction solar cells, even under ideal material and theoretical conditions, can only reach around 33.7% efficiency, as determined by the Shockley–Queisser (SQ) limit [1].

To understand the loss mechanisms behind this limit, scientists commonly use the detailed balance model, which is a general framework used to calculate the theoretical efficiency of solar cells under different conditions. It assumes: (1) photons with energy equal to or higher than the bandgap, the minimum energy required to free an electron from the valence band into the conduction band, are always absorbed, (2) the system remains in thermal equilibrium, and (3) carriers are collected regardless of where they are generated.

The Shockley–Queisser limit mainly arises from three types of losses: Thermalization losses, recombination losses, and transmission losses, as discussed in section 2.

To overcome these losses, many designs have been proposed. Among them, multijunction (MJ) solar cells [2, 3] remain the most successful in practice. These cells use multiple semiconducting layers made from different materials to absorb different portions of the solar spectrum more efficiently. To effectively absorb as much of the energy from photons as possible in a usable fashion, the cells are structured so that higher-bandgap materials are placed on top and lower-bandgap materials below.

However, MJ cells also have their limitations. Even in the most optimistic theoretical models [4], their efficiencies cannot exceed around 86.8% with infinite junctions. In addition, beyond 4 to 6 junctions, the marginal gains begin to plateau due to diminishing returns.

Another design, known as the down-converting (DC) solar cells [5], introduces a different concept: splitting a single high-energy photon into two or more lower-energy photons, which can be absorbed by lower-bandgap junctions. This technique, known as down-conversion, can, in principle, increase the number of usable photons and improve efficiency. Serveral physical processes can act as down-conversion mechaisms, including parametric down conversion [6, 7] and singlet fission [8, 9]. This paper will not cover their physical mechanisms in detail, but they are essential for future experimental designs.

Although down-conversion is promising, its practical implementation faces challenges. It is a probabilistic process because only a portion of high-energy photons undergo conversion. Moreover, engineering a material with the correct bandgap alignment and compatibility with photovoltaic architectures is not a trivial task. Common materials studied for this purpose include pentacene and tetracene [9, 10], both of which exhibit consistent down-conversion behavior.



In this work, we explore the theoretical benefit of combining DC layers with MJ cells. We model a system using a detailed balance framework and implement a differential evolution algorithm to find the optimal bandgaps for each combination of junctions and down-conversion layers. Our model predicts a theoretical peak efficiency of 63.8%, surpassing the Shockley–Queisser limit and outperforming conventional MJ cells. We also examine the number of layers required before diminishing returns set in.

Lastly, we discuss the potential engineering and fabrication challenges associated with creating such hybrid devices and suggest future directions, including the possibility of combining down-conversion and up-conversion [11, 12] to push the efficiency boundary even further.

2 Theoretical Framework

We begin by constructing a mathematical representation of the down-converting MJ solar cell (DC-MJ). At its core, the operating principle of a solar cell is simple: when incoming radiation strikes the p-n junction with enough energy, electrons are excited across bandgap. The result is the creation of a quasiparticle known as an exciton, a bound electron-hole pair. If the exciton reaches the depletion region, it separates as a result of the built-in electric field, generating free carriers. These carriers flow through an external circuit, producing current and delivering power to a connected load.

However, in reality, many processes are difficult to account for. These include non-ideal material defects and recombination mechanisms. To simplify the problem, we use the detailed balance model [1], which is based on the following assumptions: (1) photons with energy equal to or greater than the bandgap are always absorbed, (2) the cell is in thermodynamic equilibrium, (3) carriers contribute to the current regardless of where they are generated, and (4) spontaneous emission is the only form of recombination loss considered.

We begin with the single-junction model, and then generalize it to include down-conversion and MJ structures.

2.1 Single-Junction Cell

From [13], we know that the equations to model the detailed balance model for a single junction are as follows: The photogenerated current is given by:

$$J_g(E_g) = q \int_{E_g}^{\infty} \gamma \, \phi(E) dE \tag{1}$$

where q is the elementary charge in Coulomb, Eg is the energy of the bandgap in electron volts, γ is the carrier multiplication factor, which will be set to 1 in the review, and $\phi(E)$ is the photon flux, which in this review will be a manipulation of the irradiance recorded in the AM1.5G spectrum [14].

Assuming spontaneous emission is the only recombination mechanism, the recombination current is governed by generalized blackbody radiation:

$$J_r(E_g) = \frac{2\pi q^4}{c^2 h^3} \int_{E_g}^{\infty} \frac{E^2}{\exp\left(\frac{E - \gamma V}{kT}\right) - 1} dE$$
 (2)

where c is the speed of light in a vacuum in meters per second, h is the Planck constant in electron volts-second, k is the Boltzmann constant in electron volt per Kelvin, T is the temperature of the cell in Kelvin, and V is the voltage of the cell in volts.

Thus the total current is:

$$J_{total}(E_g) = J_g(E_g) - J_r(E_g)$$
(3)

To find the power of the cell P_{cell} , we determine the voltage that maximizes the product of V and J_{total} over all voltages between 0 and the open-circuit voltage V_{oc} .

 V_{oc} is the maximum voltage available from a solar cell, occurring when the net current is zero. By modifying the ideal diode equation [1] and setting the net current to zero, we obtain:

$$V_{oc}(E_g) = \frac{nkT}{q} \ln(\frac{J_g(E_g)}{J_r(E_g)} + 1)$$
(4)

And the conversion efficiency becomes:

$$\eta = \frac{P_{cell}}{P_{in}} \tag{5}$$

where input power P_{in} is calculated from:

$$P_{in} = q \int_0^\infty E_g \,\phi(E) \tag{6}$$

This was then repeated for bandgaps ranging from 0 eV to 5 eV and shown in Figure 1. The theoretical maximum efficiency for a single-junction cell is 33.7%, achieved at a bandgap of 1.34 eV.

Solar Cell Efficiency Breakdown and Loss Mechanism

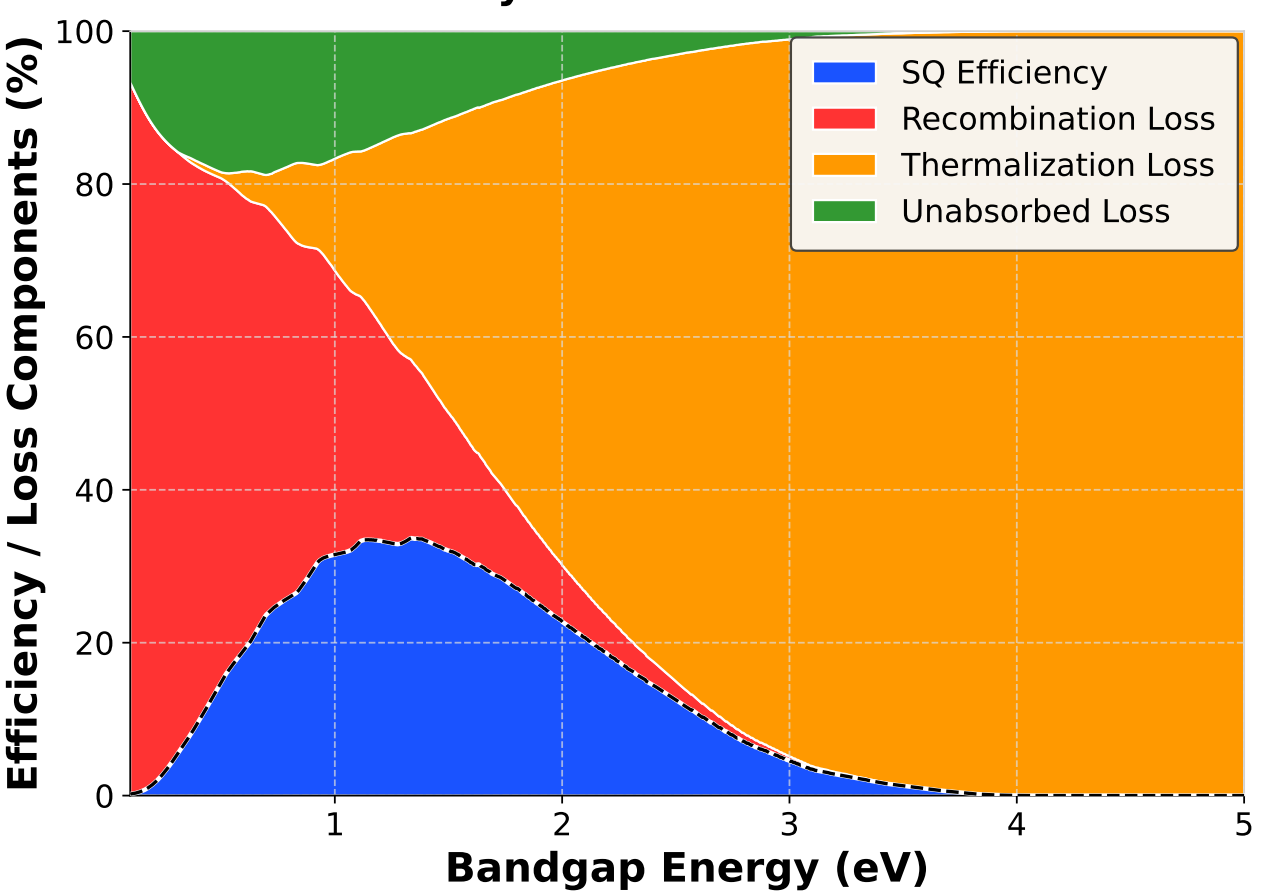


Figure 1: Theoretical efficiency of a single-junction solar cell as a function of bandgap energy, calculated using the detailed balance model assuming ideal conditions. The maximum efficiency of approximately 33.7% occurs near a bandgap of 1.34 eV, consistent with the Shockley–Queisser limit [1].

2.2 Loss Mechanisms

There are three primary losses in such idealized conditions which affects the single-junction efficiency: (1) Recombination losses, including radiative and non-radiative processes, where electrons recombine



with holes instead of generating power; (2) thermalization losses, where excess photon energy is lost as heat when high-energy electrons relax to the band edge; and (3) transmission losses, where photons with energy below the bandgap are not absorbed and pass through the cell.

Among these, recombination losses are typically divided into two broad categories: radiative and non-radiative recombination. In simple terms, recombination occurs when an electron in the conduction band relaxes back to the valence band and recombines with a hole, releasing the energy of the absorbed photon instead of converting it into electrical power.

Radiative recombination, also known as band-to-band recombination, is the most fundamental type of loss. When an electron recombines with a hole, it emits a photon with energy equal to or less than the bandgap. This photon escapes the cell, meaning its energy is lost to the system.

Non-radiative recombination, which is not considered in the SQ limit, encompasses several additional processes in which no photon is emitted. Auger recombination occurs in a system with three or more charge carriers. After electron—hole recombination, the released energy is transferred to a third carrier in the conduction band. That carrier quickly loses the excess energy as heat via phonon interactions and returns to the conduction band edge. Shockley—Read—Hall recombination (SRH) arises from defects or impurities that introduce trap states within the bandgap. An excited electron, or hole, can be captured by such a trap, and if an oppositely charged carrier is captured at the same trap before the first one relaxes, the two recombine and the energy is lost. Surface recombination occurs at the semiconductor's surface, where numerous unsatisfied bonds, known as dangling bonds, create localized states that hinder carrier motion. These surface states increase the probability of recombination for carriers generated near the surface.

Each of these recombination processes reduces the number of carriers available for current generation, thereby impacting the overall efficiency of the solar cell.

2.3 Down Conversion as a Loss-Mitigation Strategy

In principle, down-conversion can mitigate certain loss channels in photovoltaic devices. By splitting a high-energy photon into two lower-energy photons, the excess energy that would otherwise be lost to thermalization in a high-bandgap cell can instead be redistributed to lower-bandgap junctions. This can simultaneously improve spectral utilization and reduce unabsorbed photon losses in the lower junctions.

In an ideal case, the process allows a high-bandgap top cell to operate closer to its optimal voltage while still enabling the subcells below to capture additional photons. Practical limitations of the process, such as incomplete quantum yield, imperfect spectral matching, and reabsorption, are discussed in Section 5.

2.4 Multiple Junctions Usage as a Loss-Mitigation Strategy

MJ cells reduce fundamental losses by dividing the solar spectrum into narrower bands, each of which is absorbed by a subcell optimized for that specific range. This spectral splitting significantly reduces thermalization losses compared to single-junction cells, as excess photon energy above the bandgap is minimized. Additionally, transmission losses are reduced since photons that pass through higher-bandgap junctions are absorbed by lower-bandgap subcells below.

However, the design requires careful current matching between junctions and introduces fabrication complexities, including lattice matching and interface recombination issues. Despite these challenges, MJ architectures have demonstrated efficiencies exceeding single-junction limits and remain a key strategy in photovoltaic research.

3 Model Setup

3.1 Overview

The computational model is designed to simulate the theoretical performance of a DC-MJ cell under the AM1.5G spectrum, using the detailed balance framework established in Section 2. The model integrates both spectral manipulation to account for DC layers and MJ efficiency calculations, followed by an optimization procedure to identify configurations with the highest theoretical efficiency.



3.2 Spectrum Modification for Down-Conversion

The first step in the simulation is to apply the down-conversion effect to the reference AM1.5G spectrum. For any incident photons with energy equal to the DC layer's bandgap, we assume: (1) quantum efficiency = 100%, or all photons with the right energy undergo down-conversion; (2) no partial conversion losses, or the process is ideal; and (3) photons are re-emitted at half the original bandgap's energy, within ± 50 meV.

This is implemented by removing all irradiance contributions within ± 50 meV of the layer's bandgap from the spectrum [15], and adding the equivalent photon flux back at the down-converted energy bin, which is half the original bandgap, with the same ± 50 meV spread.

This spectral manipulation is applied before any cell integration or current calculations, ensuring that subsequent efficiency estimates reflect the altered photon distribution.

3.3 Multijunction Integration

To simulate MJ cells, we modify the bounds of integration in Equation (1). Instead of integrating from the bandgap to infinity, each junction integrates from its bandgap to the next higher bandgap above it. The topmost cell integrates from its bandgap to infinity.

This process ensures that each junction receives only the photons within its assigned energy range, as dictated by its position in the stack.

The recombination current still follows Equation (2), as it depends only on the junction's bandgap.

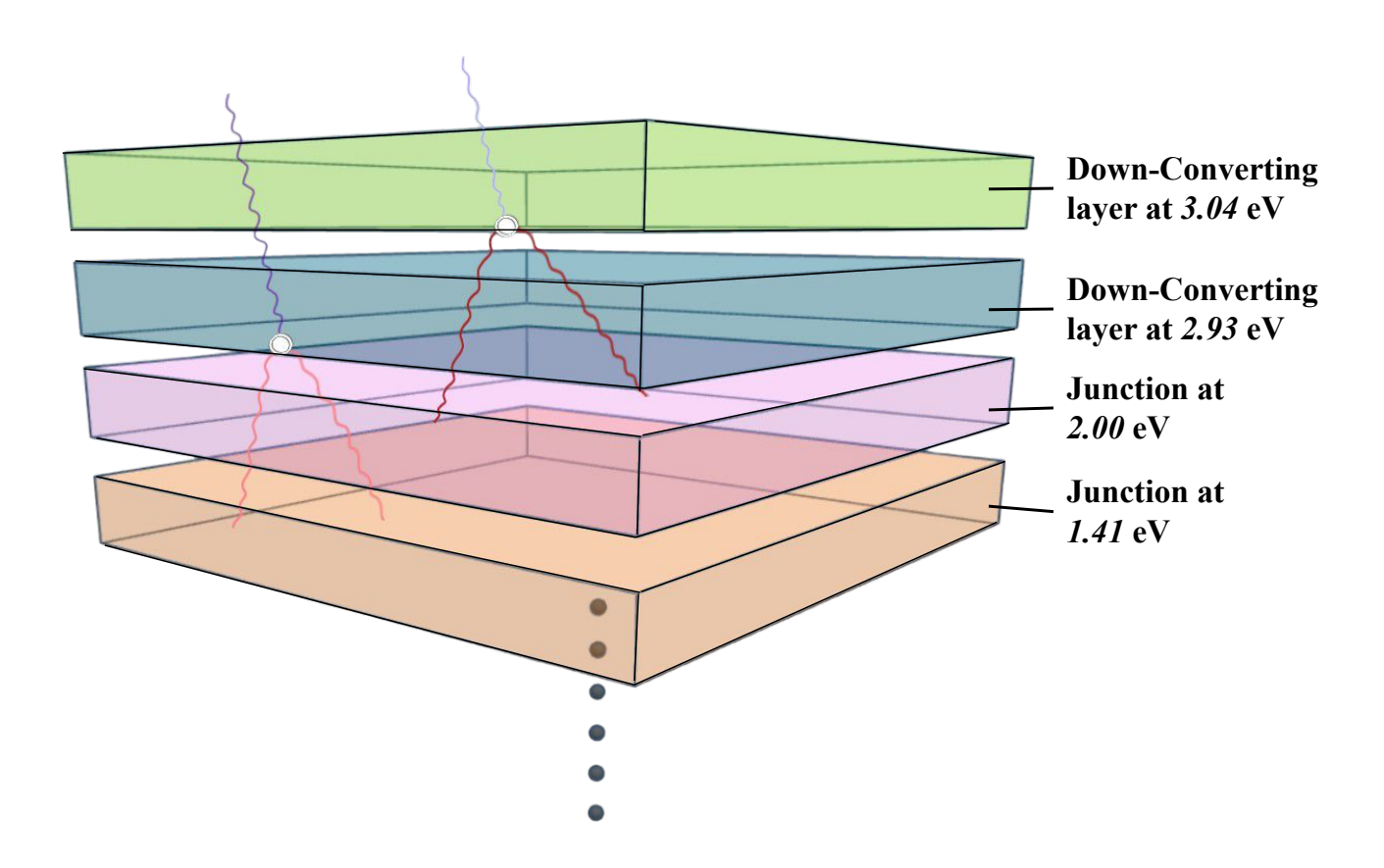


Figure 2: Schematic architecture of a DC-MJ cell, showing the arrangement of DC layers above the MJ stack.



Figure 2 illustrates the typical architecture of a DC-MJ cell, showing the arrangement of junctions and down-conversion layers as modeled in the computational framework. The modeled architecture includes two DC layers with bandgaps of 3.04 eV and 2.93 eV at the top of the stack, followed by two MJ cells with bandgaps of 2.00 eV and 1.41 eV. Additional junctions may be included as indicated in Figure 2. This arrangement is one of the optimal configurations identified in this study, as discussed in the following sections.

3.4 Optimization Procedure

The next step is to find the optimal combination of bandgaps and DC layers that maximizes efficiency. We use a differential evolution algorithm [16], a stochastic optimization method well-suited for high-dimensional, continuous parameter spaces. Unlike gradient-based methods, it is less likely to get trapped in local minima, a significant advantage here since our search space has up to 24 dimensions (bandgap energies + down-conversion layers), making the best use of computational time and resources.

Each run is initialized with a different random seed to assess result consistency. The algorithm iteratively refines candidate solutions based on a fitness function, which is chosen to be the total calculated efficiency from Equation (5). The search considers bandgaps within the range of 0 to 5.0 eV, with the constraint that bandgaps must strictly decrease from the top to bottom cell. Configurations tested range from a single junction with no DC layers up to 12 junctions with 11 DC layers, with multiple runs performed per configuration to reduce the chance of local optima.

The results are summarized in [17], with particular attention to Table 1. While we cannot guarantee a global optimum due to the stochastic nature of the method, the results consistently showed improved performance with the inclusion of down-conversion.

3.5 Output Data

The simulation outputs: (1) the optimal bandgap configurations for all tested junction and DC layer combinations, and (2) the theoretical efficiency values for each configuration.

The primary dataset used in this study is Table 1, summarizing optimal configurations across the explored parameter space.

4 Results

4.1 Bandgap Distribution without Down-Converting Layers

Using the results recorded in Table 1, we plotted the distribution of optimal bandgap combinations for configurations without any DC layers, ranging from 1 to 12 junctions shown in Figure 3.

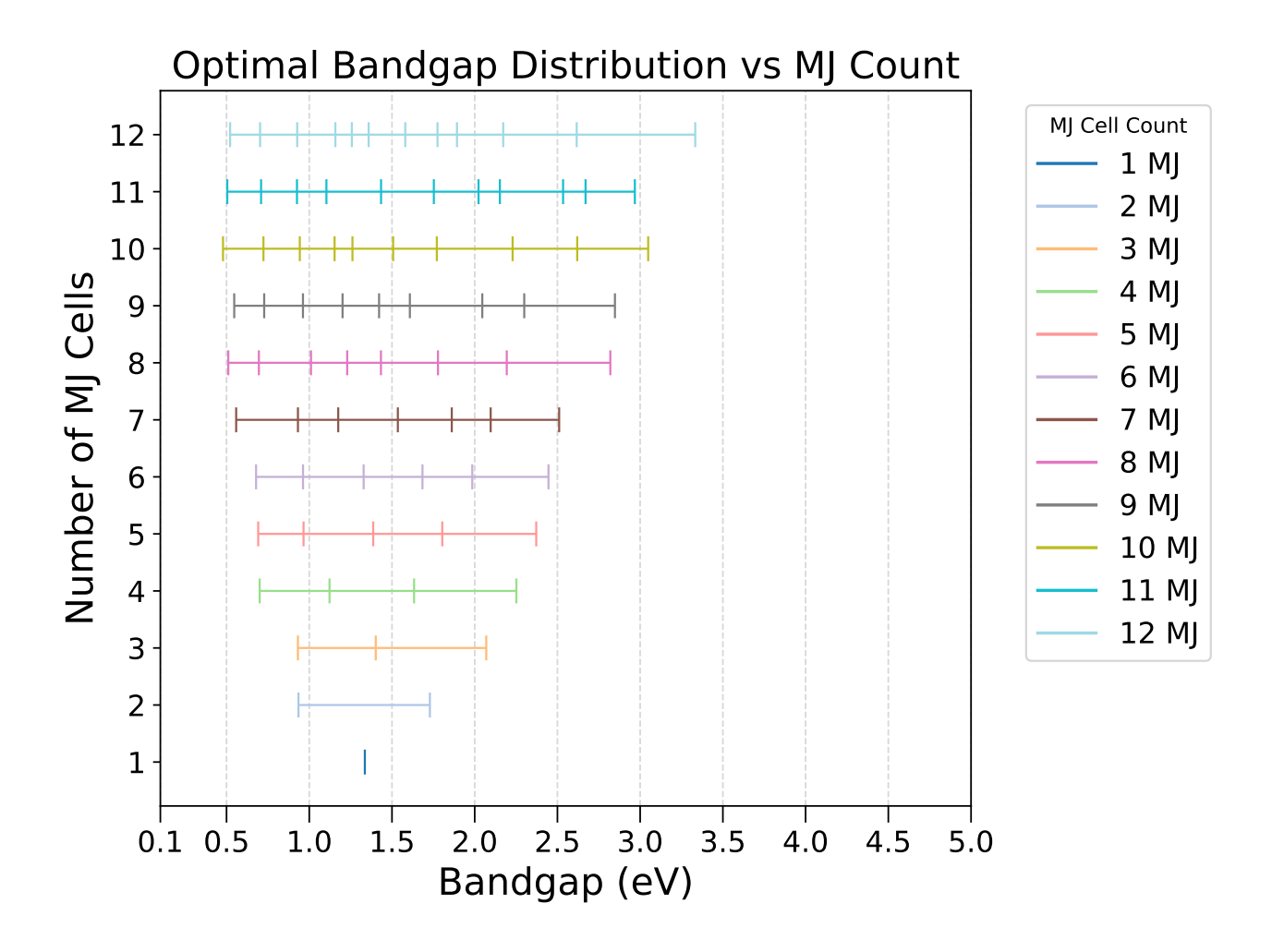


Figure 3: Distribution of optimal bandgap values for MJ solar cell configurations without DC layers, spanning 1 to 12 junctions. Bandgaps cluster predominantly between 0.5 eV and 3 eV, with closer spacing as junction count increases.

From Figure 3, we observe that although bandgaps can theoretically span from 0 to 5 eV, the optimal values are heavily concentrated between 0.5 eV and 3 eV, with a particularly dense region around 1–2 eV. As the number of junctions increases, bandgaps become more tightly spaced. This reflects how spectral segments must narrow and spread more evenly across the energy range, demanding finer bandgap resolution.

This trend underscores a fundamental trade-off: while junctions must be distinct enough to capture different parts of the spectrum, they also need to remain within the high-flux region of the solar spectrum. Hence, the algorithm converges toward the 1–2 eV region, where the balance between photon availability and voltage potential is most favorable.

This behavior is not random; it reflects the internal logic of the optimization algorithm, which prioritizes configurations that maximize efficiency under spectral constraints. Very high or very low bandgaps contribute little due to fewer available photons or reduced voltage, respectively. This distribution pattern persists across other configurations involving DC layers.

4.2 Efficiency Trends with Junctions and Down-Converting Layers

We now examine how efficiency varies as a function of both the number of MJ and DC layers.

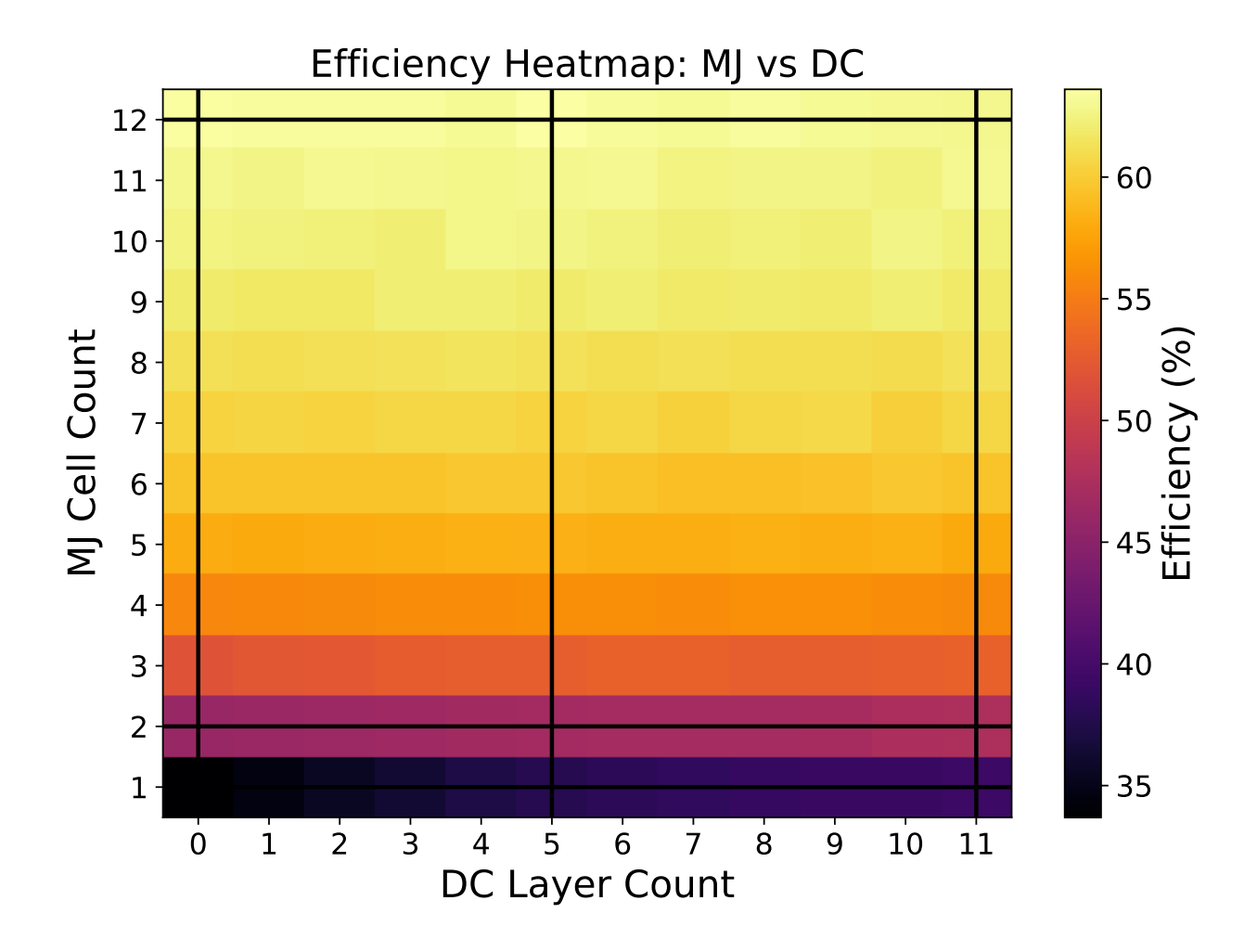


Figure 4: Heat map illustrating the theoretical efficiency of the DC-MJ cell as a function of the number of junctions and DC layers. Horizontal and vertical line cuts highlight efficiency trends along each parameter independently.

From the heat map in Figure 4, we observe two key patterns: (1) Efficiency increases consistently with the number of junctions, for any given number of DC layers, and (2) increasing the number of DC layers leads to only slight efficiency improvements, with clear diminishing returns as both parameters increase.

Horizontal and vertical line cuts have been put in the graphs to represent how the efficiency changes with respect to the number of junctions or the number of DC layers

4.3 Diminishing Returns: Junction Count Saturation

Figure 4a shows how efficiency changes as we increase the number of junctions while fixing the number of DC layers.

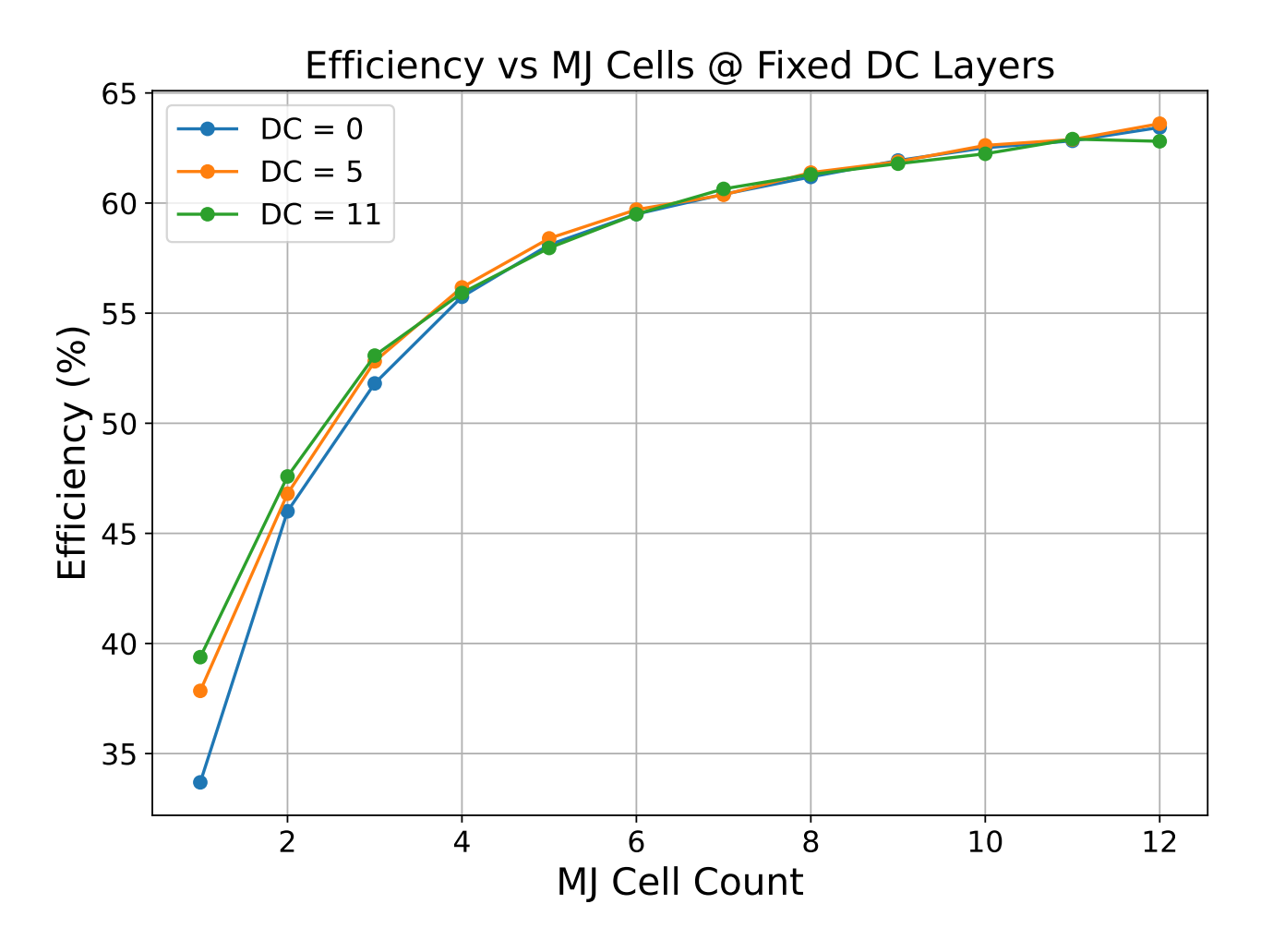


Figure 4a: Efficiency as a function of the number of junctions for fixed DC layers. Each curve corresponds to a different DC layer count.

The initial efficiency with one junction and 5 DC layers is 37.84%. At four junctions, it jumps to 56.17%. However, beyond this point, each added junction contributes less than 1.5% additional efficiency. Although the theoretical maximum (63.61%) occurs at 12 junctions and 5 DC layers, the increased complexity may not justify the minor gains.

Interestingly, in some cases, adding an additional junction can actually decrease efficiency, for example when going from 11 to 12 junctions with 11 DC layers. This decrease may result from limitations of the optimization algorithm, such as variability due to the random seed, or from physical constraints, such as oversaturation of the photogenerated current, which reduces the voltage-current product as discussed in Section 2.1. Similar patterns are observed across other random seeds.

4.4 Diminishing Returns: Down-Converting Layer Saturation

Figure 4b explores the inverse case, how efficiency changes as we increase the number of DC layers while keeping the number of junctions fixed.

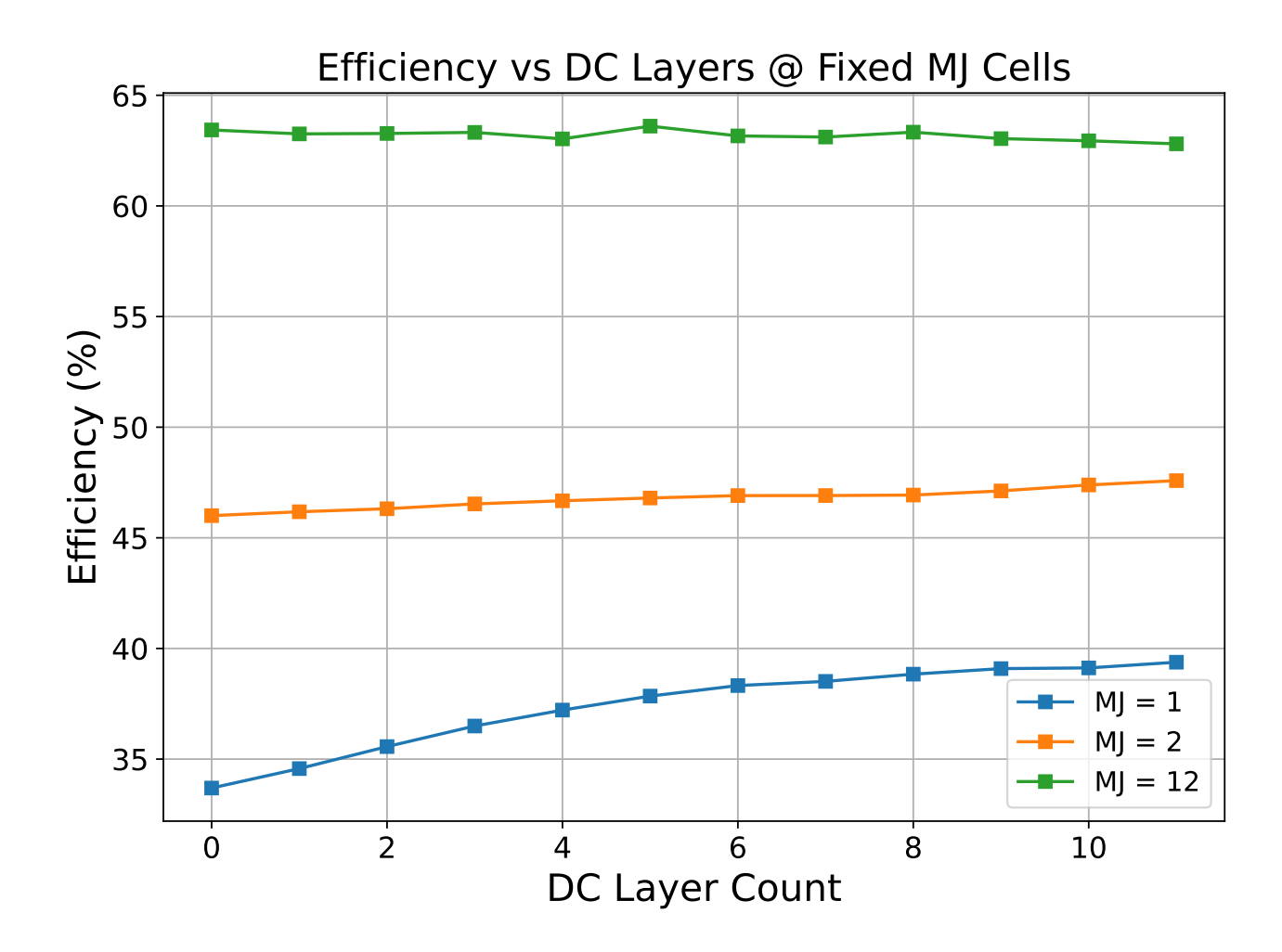


Figure 4b: Efficiency of solar cells as a function of the number of DC layers for fixed junction counts. Each curve corresponds to a different junction number.

For a single junction, the efficiency increases steadily but modestly with added DC layers. Even with 11 DC layers, the gain is only 6%. For higher junction counts, the increase becomes less predictable. For example, the 12-junction configurations show oscillations in efficiency as more DC layers are added. This further supports the idea that excessive spectral focusing narrows the irradiance too much, thereby limiting the operating voltage and reducing total efficiency.

4.5 Limits of Down-Converting: Artificial Spectrum Compression

To test the hypothesis that excessive DC might harm efficiency, we ran a simulation with 100 DC layers and one junction. The result: it only achieved an efficiency of 28.7%, lower than the baseline single-junction configuration.

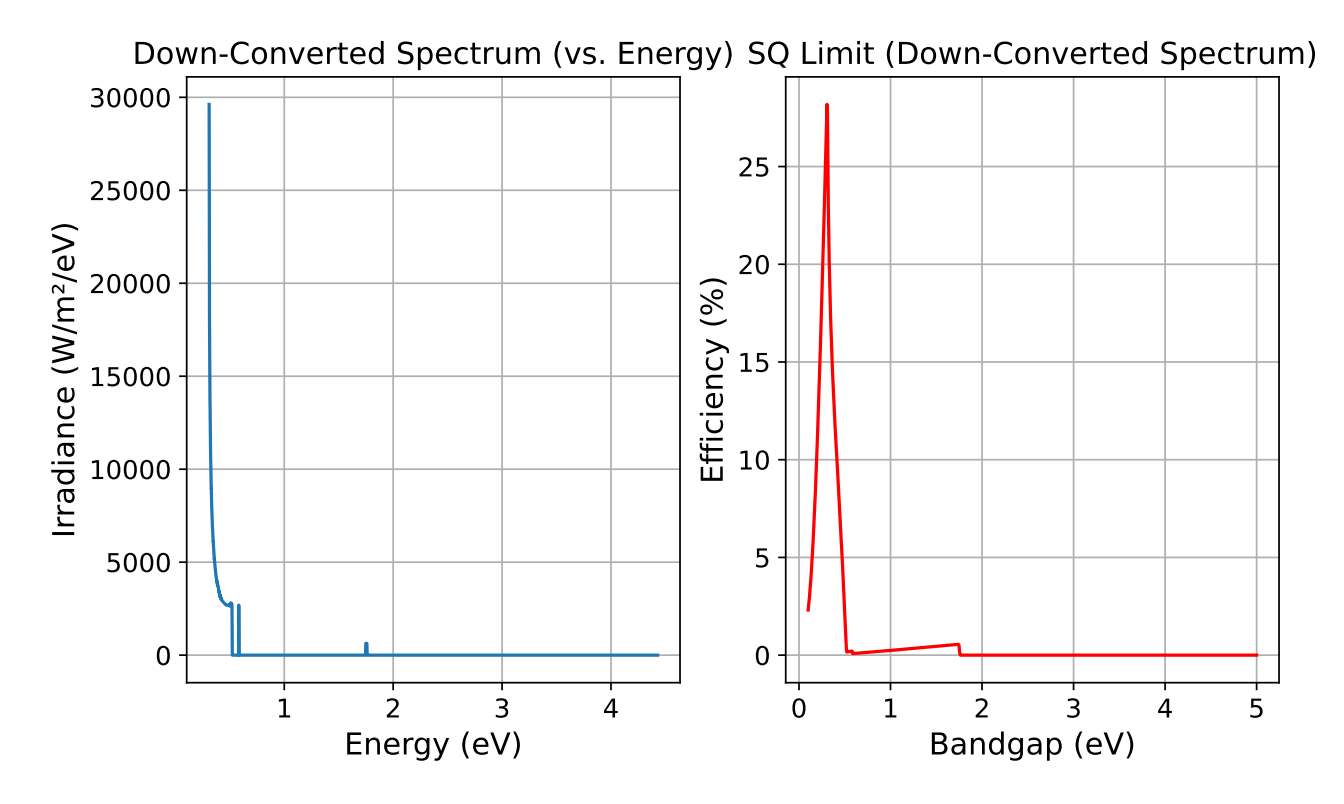


Figure 5: Simulation of a single-junction cell with 100 DC layers. The irradiance spectrum compresses into a narrow spike around 3000 W/m².

The corresponding spectrum plot shows a sharp irradiance spike, peaking at 3000 W/m², which is over 500 times the original peak of the AM1.5G spectrum. However, this extreme spectral compression leaves most neighboring energies with negligible power, drastically reducing the cell's operating voltage, and hence, overall efficiency. This confirms our earlier hypothesis: pushing photons into a narrow band is counterproductive and results in lower efficiency.

4.6 Spectrum Shaping vs Efficiency: Not Just About Peaks

Figure 6 compares spectrum modifications under different DC layer configurations.

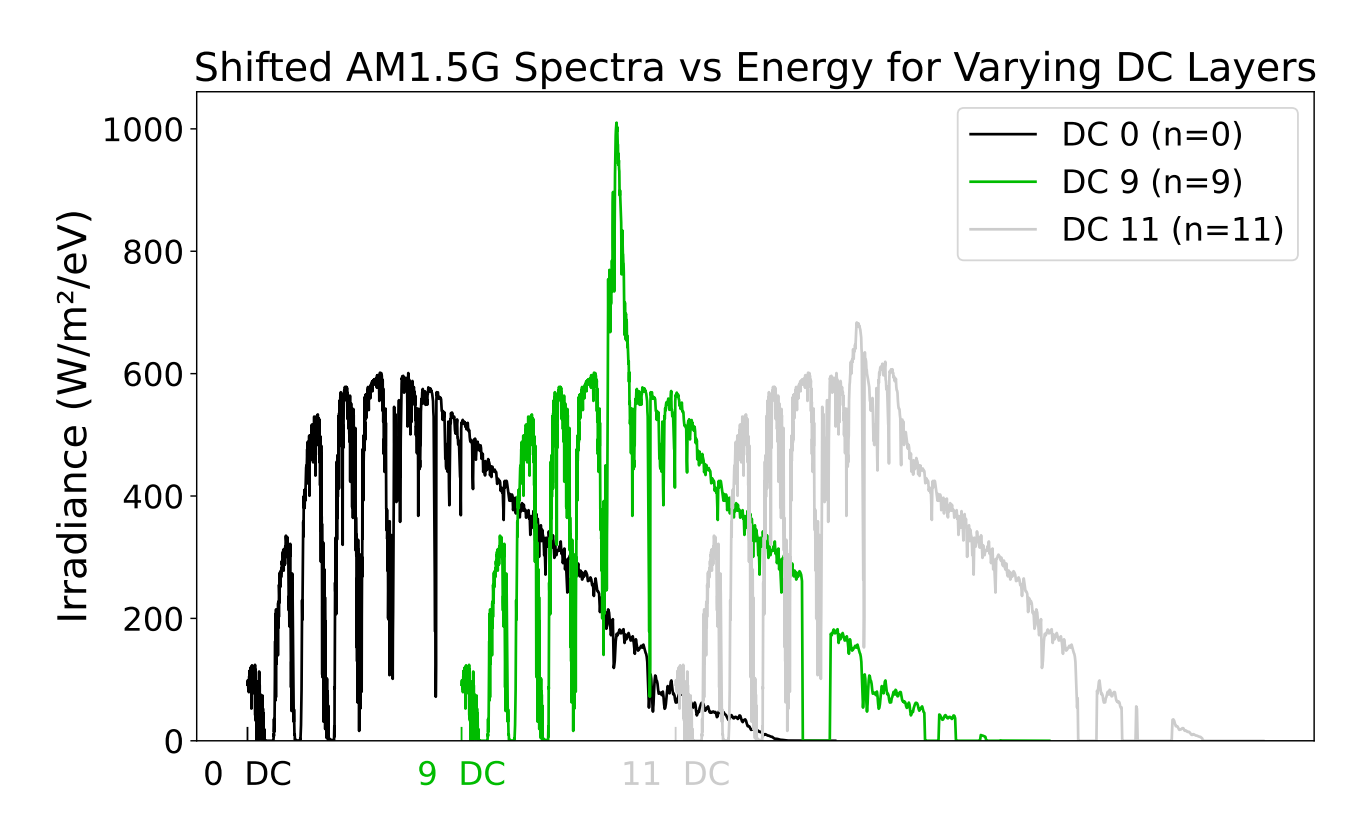


Figure 6: Spectral irradiance profiles under different DC layer configurations. The 9-DC spectrum shows a sharp peak, while the 5-DC spectrum is more evenly distributed.

The 9-DC configuration produces the highest irradiance peak, yet it does not yield the best efficiency. In constrast, the 5-DC spectrum is broader and more balanced, leading to higher performance. This reinforces the principle that efficiency is not maximized by driving photons into narrower bands to increase the effective photogenerated current at a specific point, but rather by maximizing power by striking a balance between current and voltage as discussed in section 2.1. By distributing photons across multiple bandgaps, the 5-DC case better preserves both current and voltage, achieving higher efficiency.

5 Analysis – Engineering Challenges

This section addresses the potential practical and engineering challenges of constructing a DC-MJ cell. While the assumptions in our model may appear to oversimplify the physics, this approach is common in photovoltaic research. For example, the well-known Shockley–Queisser limit neglects various thermodynamic effects and real-world defects, yet its predicted optimal bandgaps—such as those for silicon and gallium arsenide—correspond closely to the materials most widely used in commercial solar cells. This suggests that even highly idealized models can yield valuable, physically relevant predictions.

5.1 Voltage Losses Between Junctions

In our model, we assumed zero voltage losses between the MJ layers. In practice, this is rarely achievable [18]. When junctions are connected in series, the voltage of all the cells is determined by the subcell with the lowest open-circuit voltage. This means that even a single under-performing junction can limit the output of the entire device. Furthermore, integrating DC layers between junctions introduces additional connection challenges, requiring precise optical, electrical, and thermal management. Although these issues can, in principle, be addressed through advanced engineering, they are challenging to model accurately, and neglecting them in simulation will likely lead to overestimating real-world efficiencies.



5.2 Material Defects

The model assumes no efficiency losses from material defects, an idealization that is difficult to achieve in practice. Defects can severely reduce performance through mechanisms such as Auger recombination or surface recombination as outlined in Section 2.2). Advanced fabrication methods, such as Molecular Beam Epitaxy [19], can create materials with exceptionally low defect densities by growing them layer-by-layer in an ultra-high vacuum, minimizing contamination. If the cells for this design are constructed using this technique, these loss mechanisms can be reduced significantly, allowing the cells to reach higher efficiencies. However, the required equipment can cost millions of dollars, making large-scale adoption economically challenging and slowing progress in solar cell development.

5.3 Material Bandgap Tunability

The model assumes complete control over the bandgap of each subcell material, a capability that is currently limited [20]. While it is theoretically possible to manufacture materials with arbitrary bandgaps, achieving the exact values predicted by the optimization algorithm is technologically challenging. Recent developments in perovskite materials, which exhibit highly tunable bandgaps due to their diverse chemical compositions, offer a promising pathway toward this goal. Although perfect precision remains elusive, advances in synthesis and compositional engineering suggest that near-ideal bandgap tuning could become feasible in the near future.

5.4 Realistic Down-Conversion Efficiencies

Our simulations treated each down-converter as having 100% quantum efficiency, meaning that every photon at the appropriate energy is perfectly split into two lower-energy photons. In reality, no material achieves this level of performance.

Two widely studied down-conversion mechanisms introduced in section 1 included: (1) Parametric Down-Conversion (PDC), this process occurs in nonlinear optical crystals with nonzero second-order susceptibility, $\chi^{(2)}$ [21], which is ultimately governed by the crystal's dielectric tensor. In PDC, high-energy incident photon, known as the pump photon, is split into two lower-energy photons, known as the daughter photons, that together conserve both energy and momentum. These requirements, known as the phase-matching conditions, are only satisfied within very narrow wavelength ranges that are often less than 1 nanometer and for carefully aligned crystal orientations. Because the solar spectrum is broadband, only a small fraction of incident sunlight can be converted in practice, even before losses from scattering, absorption, or limited coherence are considered. (2) Singlet Fission (SF), which occurs in certain organic semiconductors such as pentacene and tetracene, can split a single high-energy singlet exciton into two lower-energy triplet excitons, if $E_{S1} \geq 2E_{T1}$, and that the environment facilitates spin-allowed transitions [9]. Reported triplet yields can reach 50-80% in optimized films, but real devices suffer from losses such as triplet-triplet annihilation, incomplete exciton separation, and energy loss due to interference with the lattice of the material.

Both mechanisms face significant material and device-level challenges before approaching the idealized efficiencies assumed in our model.

5.5 Algorithmic Limitations and Unrealistic Bandgaps

The optimization algorithm occasionally identified bandgap configurations that are impractically close, within 5 meV of each other, which effectively corresponds to the same material. In the results recorded in Table 1, several configurations exhibited this issue, including [5DC, 8MJ], [5DC, 12MJ], [8DC, 12MJ], [10DC, 1MJ], [10DC, 5MJ], and [10DC, 9MJ].

Although these configurations remain valid theoretical optima under the model assumptions, they are not physically realizable without additional constraints. Introducing such constraints directly into the algorithm could yield more realistic designs, but may also prevent the discovery of the absolute theoretical optimum.



5.6 Summary of Practical Implications

Although our simulations illustrate the maximum possible performance of DC–MJ cells, several practical realities will lower the efficiencies that can be achieved in practice. Series connections between junctions inevitably introduce voltage bottlenecks, making the overall output dependent on the weakest subcell. Bandgap tunability, while improving rapidly, particularly in pervoskites, still remains challenging to perfectly match the spectra predicted by optimization. Similarly, down-conversion mechanisms such as parametric down-conversion or singlet fission still operate far below unity quantum efficiency, even under optimized conditions. Finally, the optimization algorithm occasionally identifies bandgap sets that are not physically realizable, highlighting the gap between mathematical idealization and material feasibility.

Nevertheless, these challenges should not be interpreted as impossible barriers. Progress in materials science and device engineering continues to narrow the distance between theoretical models and experimental practice. As fabrication techniques mature and novel semiconductors emerge, it is plausible that future devices could capture many of the advantages suggested by the present study, moving closer to the idealized limits outlined here.

6 Future Work - Up-Conversion and Conclusion

6.1 Up-Conversion as a Complement to Down-Conversion

A promising route to further increase the efficiency of the proposed system is to incorporate up-converting (UC) layers alongside the DC layers. Up-conversion operates as the inverse of down-conversion: instead of splitting a high-energy photon into two lower-energy photons, UC combines two or more lower-energy photons into a single photon of higher energy.

The primary advantage of UC is its ability to mitigate thermalization losses, particularly significant at lower bandgaps, by converting sub-bandgap photons that would otherwise be wasted into photons that can be absorbed. Similar to how DC reduces losses from unabsorbed high-energy photons, the combination of UC and DC placed at distinct regions of the solar spectrum could theoretically optimize both major loss channels in MJ photovoltaics. This expanded spectral utilization is expected to yield efficiencies exceeding those achievable by DC-only architectures.

6.2 Modeling UC in the Existing Framework

In our theoretical model, up-conversion is incorporated by extending the mathematical treatment used for down-conversion, effectively combining photon energies rather than splitting them. While down-conversion splits high-energy photons into two lower-energy photons, up-conversion combines two or more lower-energy photons into a single higher-energy photon, enabling the cell to utilize sub-bandgap photons that would otherwise be lost.

To explore the potential benefits of combining UC and DC within MJ cells, we applied the differential evolution (DE) optimization algorithm to search for optimal bandgap configurations of up-down-converting multijunction (UDC-MJ) cells. This approach allows simultaneous optimization of junction energies and conversion layer arrangements, identifying configurations that maximize overall theoretical efficiency.

The DE algorithm identified an optimal configuration achieving an impressive theoretical efficiency of 69.2%, consisting of 11 junctions, 2 down-conversion layers, and 9 up-conversion layers. This result significantly surpasses efficiencies predicted for cells with only down-conversion or only up-conversion layers, highlighting the synergistic potential of combining both mechanisms.

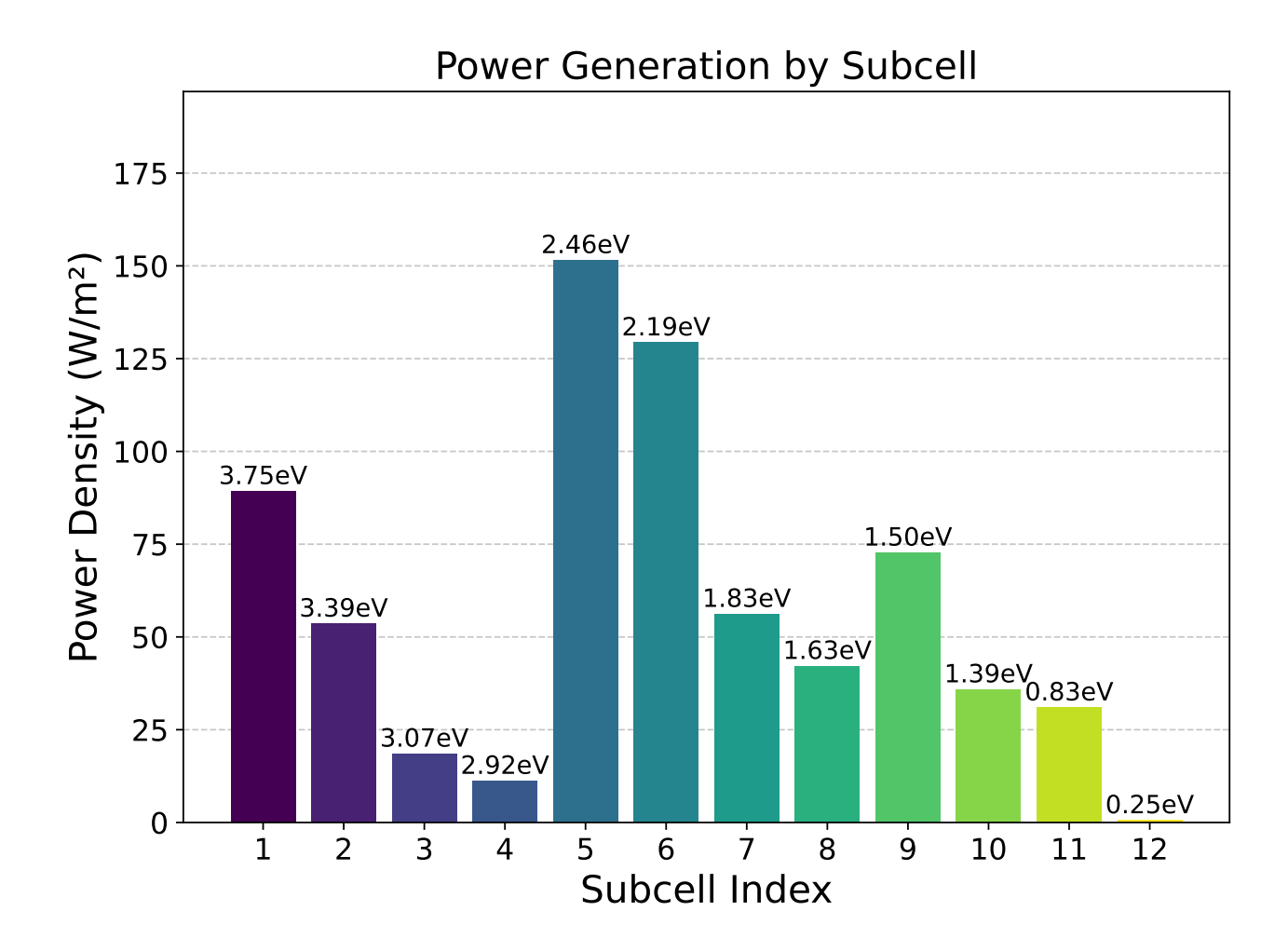


Figure 7: Power density distribution across the junctions in the optimal UDC-MJ configuration after spectral modifications by up-conversion and down-conversion layers.

Figure 7 illustrates the irradiance profile after spectral modifications induced by the optimal UC and DC layers. The distribution of power density among the junctions is relatively even, ranging from approximately 50 to 150 W/m² per cell. This balance in power density is crucial, as optimal configurations tend to avoid overloading any single junction, instead spreading the spectral power more uniformly to maximize combined output.

Interestingly, preliminary results suggest that configurations employing only UC layers (without DC) can already outperform many of the best DC-MJ cells in terms of theoretical efficiency. Incorporating both UC and DC layers further enhances performance, as demonstrated by the configurations explored by the DE algorithm (Table 3, [17]).

These findings underscore the importance of considering both up- and down-conversion processes in the design of advanced solar cells. While practical implementation challenges remain, such as achieving high quantum efficiencies and effective coupling between layers, the theoretical framework provides a promising direction for pushing solar cell efficiencies beyond traditional limits.

6.3 Practical Considerations for UC Implementation

As with DC–MJ cells, integrating UC layers into the devicepresents significant engineering challenges, many of which are similar to those mentioned earlier. However, the bandgap tunability of UC layers is often better due to the materials employed. Examples include quantum dots, which offer high tunability and broad design flexibility through chemical composition or size control [22]; nonlinear crystals with strong second-harmonic generation (a $\chi^{(2)}$ term in the dielectric tensor) [23]; and lanthanide-doped phosphors,



which are well known for multi-photon up-conversion via intermediate electronic states [24]. These materials exhibit varying trade-offs between tunability, spectral coverage, and conversion efficiency. While some have demonstrated promising performance in laboratory settings, none yet achieved the unity quantum efficiency assumed in our theoretical model.

6.4 Conclusion

In this work, we proposed and analyzed a new photovoltaic architecture, the down-converting multijunction solar cell, and explored the potential for further efficiency gains through the inclusion of upconversion layers. Using a detailed balance framework and a differential evolution optimization algo-

rithm, we determined the maximum theoretical efficiencies for a variety of configurations.

Our results indicate that a 12-junction DC-MJ system can theoretically reach efficiencies near 64% under idealized assumptions. Efficiency gains from down-conversion alone are modest but measurable, with diminishing returns becoming pronounced beyond 5–6 subcells. Incorporating up-conversion into the system produces a notable efficiency boost, in some cases surpassing any DC-only configuration. For practical implementation, configurations with 2–5 subcells combined with 2–4 conversion layers, whether UC, DC, or mixed, appear to offer the best trade-off between efficiency and architectural complexity. Achieving these designs experimentally will require near-perfect bandgap tunability, a challenge that may be addressed by emerging materials such as perovskites for the photovoltaic cells, pentacene or tetracene for down-conversion, and quantum dots for up-conversion.

Future research should focus on experimentally validating UC–DC–MJ designs, developing scalable fabrication techniques for multi-layer architectures with precise bandgap control, and refining the optimization model to incorporate realistic material constraints, optical coupling losses, and thermal management. With continued progress in tunable materials and photonic engineering, the theoretical performance levels presented here may become achievable, paving the way for the next generation of ultra-high-efficiency solar cells.

Acknowledgments

We would like to thank Dr. Aaron R. Altman for the guidance along the project.

References

- [1] W. Shockley and H. Queisser, in *Renewable Energy* (Routledge, 2018) pp. Vol2_35–Vol2_54.
- [2] E. D. Jackson, in *Trans. Intern. Conf. on the Use of Solar Energy The Scientific Basis*, Vol. 5 (1955).
- [3] S. M. Bedair, M. F. Lamorte, and J. R. Hauser, Applied Physics Letters 34, 38 (1979).
- [4] A. De Vos, Journal of Physics D: Applied Physics 13, 839 (1980).
- [5] T. Trupke, M. A. Green, and P. Würfel, Journal of Applied Physics 92, 1668 (2002).
- [6] D. Magde and H. Mahr, Physical Review Letters 18, 905 (1967).
- [7] D. N. Klyshko, ZhETF Pisma Redaktsiiu 6, 490 (1967).
- [8] M. Pope and C. E. Swenberg, Annual Review of Physical Chemistry 35, 613 (1984).
- [9] R. P. Groff, P. Avakian, and R. E. Merrifield, Journal of Luminescence 1, 218 (1970).
- [10] J. H. Perlstein, Chemical Physics Letters 4, 707 (1969).
- [11] F. Auzel, Journal of Luminescence 45, 341 (1990).
- [12] C. A. Parker, Transactions of the Faraday Society 60, 1998 (1964).



- [13] F. H. Alharbi and S. Kais, Renewable and Sustainable Energy Reviews 43, 1073 (2015).
- [14] National Renewable Energy Laboratory, Reference solar spectral irradiance: Air mass 1.5, https://www.nrel.gov/grid/solar-resource/spectra.html (2012), u.S. Department of Energy.
- [15] S. Refaely-Abramson et al., Physical Review Letters 119, 267401 (2017).
- [16] R. Storn and K. Price, Journal of Global Optimization 11, 341 (1997).
- [17] Y. Lui, Down-converting multijunction solar cell, https://github.com/Yalurtyi/Down-Converting-Multijunction-Solar-Cell (2025).
- [18] I. M. Peters et al., Progress in Photovoltaics: Research and Applications 31, 1006 (2023).
- [19] A. Y. Cho and J. R. Arthur, Progress in Solid State Chemistry 10, 157 (1975).
- [20] M. H. Miah et al., RSC Advances 14, 15876 (2024).
- [21] R. W. Boyd, Nonlinear Optics, 3rd ed. (Academic, Burlington, 2008).
- [22] N. T. Mamedov et al., Journal of Luminescence **72–74**, 217 (1997).
- [23] P. A. Franken et al., Physical Review Letters 7, 118 (1961).
- [24] F. Auzel, Chemical Reviews 104, 139 (2004).